In Vivo Quantification of Peroxisome Tethering to Chloroplasts in Tobacco Epidermal Cells Using Optical Tweezers[1][OPEN]

Hongbo Gao, Jeremy Metz[2], Nick A. Teanby[2], Andy D. Ward, Stanley W. Botchway, Benjamin Coles, Mark R. Pollard[3], and Imogen Sparkes*

Biosciences, University of Exeter, Exeter EX4 4QD, United Kingdom (H.G., J.M., I.S.); School of Earth Sciences, University of Bristol, Clifton, Bristol BS8 1RJ, United Kingdom (N.A.T.); and Central Laser Facility, Science and Technology Facilities Council, Didcot, Oxon OX11 0FA, United Kingdom (A.D.W., S.W.B., B.C., M.R.P.)

ORCID IDs: 0000-0002-8099-8776 (J.M.); 0000-0002-3268-9303 (S.W.B.).

Peroxisomes are highly motile organelles that display a range of motions within a short time frame. In static snapshots, they can be juxtaposed to chloroplasts, which has led to the hypothesis that they are physically interacting. Here, using optical tweezers, we tested the dynamic physical interaction in vivo. Using near-infrared optical tweezers combined with TIRF microscopy, we were able to trap peroxisomes and approximate the forces involved in chloroplast association in vivo in tobacco (*Nicotiana tabacum*) and observed weaker tethering to additional unknown structures within the cell. We show that chloroplasts and peroxisomes are physically tethered through peroxules, a poorly described structure in plant cells. We suggest that peroxules have a novel role in maintaining peroxisome-organelle interactions in the dynamic environment. This could be important for fatty acid mobilization and photorespiration through the interaction with oil bodies and chloroplasts, highlighting a fundamentally important role for organelle interactions for essential biochemistry and physiological processes.

A combination of genetically encoded fluorescent probes, advances in light microscopy, and interdisciplinary approaches has revolutionized our understanding of organelle transport. Organelle movement in highly vacuolated leaf epidermal cells appears erratic, with individual organelles undergoing a range of movements within a relatively short time frame: they stop-go, change direction (trajectory), and move at varying speeds. The use of pharmacological inhibitors indicated a role for actin, and therefore myosins, in this process; however, myosin-organelle specificity is poorly characterized (Madison and Nebenführ, 2013; Tamura et al., 2013; Buchnik et al., 2015). Therefore, we are still at a relatively rudimentary stage in the understanding of the molecular and physical control, and interaction, of organelles in plant cells compared with that known in other model systems (Hammer and Sellers, 2012; Prinz, 2014). However, it is clear that organelle movement plays important roles in physiological processes in plants; reduced movement effects growth and development, and movement is correlated with responses to extracellular stresses such as pathogens and heavy metals (for refs., see Sparkes, 2011; Madison and Nebenführ, 2013; Buchnik et al., 2015). Organelle interactions in other systems have important roles in calcium and lipid exchange, setting a precedent for physiologically important roles in plants (Prinz, 2014). However, characterization of the molecular factors required to physically tether organelles, as opposed to those that function in the exchange of molecules at the interaction site, is challenging. Monitoring organelle interactions in highly vacuolated plant epidermal cells is further complicated by the constraints imposed by the large central vacuole. Static snapshots provided through electron microscopy of highly vacuolated cells,

[1] This work was supported by the Biotechnology and Biological Sciences Research Council (grant no. BB/I006184/2 to I.S. and H.G.), by an STFC user access facility grant (grant no. LSP907 to I.S. and H.G.), and by a Wellcome Trust Institutional Strategic Support Award (grant no. WT097835MF to J.M.).

[2] These authors contributed equally to the article.

[3] Present address: Dansk Fundamental Metrologi A/S, Matematiktorvet 307, Kongens Lyngby, Denmark 2800.

* Address correspondence to i.sparkes@exeter.ac.uk.

The author responsible for distribution of materials integral to the findings presented in this article in accordance with the policy described in the Instructions for Authors (www.plantphysiol.org) is: Imogen Sparkes (i.sparkes@exeter.ac.uk).

Experiments were conceived by I.S. and experimental data generated by H.G. and I.S.; A.D.W., S.W.B., B.C., and M.R.P. built, customized, maintained, and facilitated the use of the optical trap-TIRF system; experimental design was discussed with H.G., A.D.W., S.W.B., and J.M.; A.D.W. calibrated the system and performed bead-trapping experiments; H.G. performed all ImageJ analyses; J.M. wrote the tracking algorithm to generate the displacement values for N.A.T.; visual confirmation of tracking was carried out by J.M., H.G., and I.S.; N.A.T. applied the simple model of a viscously damped sphere on a spring to determine the forces involved in the system; I.S. wrote the article with comments from all authors; N.A.T. wrote Supplemental Note S1; N.A.T. and A.D.W. were involved in writing the section relating to forces.

[OPEN] Articles can be viewed without a subscription.

www.plantphysiol.org/cgi/doi/10.1104/pp.15.01529

where the vacuole can effectively push organelles together, giving the impression of direct interaction between organelles, is not a suitable method to determine dynamic interactions. Other techniques, such as the laser-induced shockwave by explosion method used by Oikawa et al. (2015), works globally without directly manipulating the individual organelle. Here, using optical tweezers with submicron precision, we provide a means to assess and quantify the dynamic interaction between peroxisomes and chloroplasts in vivo in leaf epidermal cells.

Peroxisomes are responsible for several biochemical reactions, including the glyoxylate cycle and β-oxidation, which provides an energy source for germination in oilseeds. They also produce and scavenge free radicals, synthesize jasmonic acid and indole-3-acetic acid, and are required for photorespiration (for refs., see Hu et al., 2012). The photorespiratory pathway spans peroxisomes, chloroplasts, and mitochondria, where phosphoglycolate produced in the chloroplast is converted back to 3-phosphoglycerate. It has been suggested that functional connectivity between these organelles accounts for the close association observed in ultrastructural micrographs (Frederick and Newcomb, 1969). Several Arabidopsis (*Arabidopsis thaliana*) *pex10* (peroxisomal membrane protein) mutants show altered chloroplast-peroxisome juxtaposition with a defect in photorespiration, while others do not (Schumann et al., 2007; Prestele et al., 2010). Both CLUMPED CHLOROPLASTS1 (CLMP1) and CHLOROPLAST UNUSUAL POSITIONING1 (CHUP1) encode for proteins that localize to the chloroplast, with CHUP1 playing a role in chloroplast-actin formation (Oikawa et al., 2003, 2008; Schmidt von Braun and Schleiff, 2008; Yang et al., 2011). While CHUP1 and CLMP1 affect chloroplast positioning, they have differential effects on peroxisome and mitochondrial location; *clmp1* causes chloroplast clustering without affecting mitochondria or peroxisome location (Yang et al., 2011), whereas *chup1* was reported to affect peroxisome location (Oikawa et al., 2003). In vitro analysis through density centrifugation highlighted chloroplast sedimentation with peroxisomes under certain conditions (Schnarrenberger and Burkhard, 1977), although this does not necessarily reflect the organelle interaction in live cells. Peroxisome proteomics studies have been hampered by difficulties in isolating pure peroxisomal fractions (Bussell et al., 2013). This could be indicative of interaction, where associated membranes are isolated together, or sticky nonspecific contaminating chloroplast membranes. The work by Oikawa et al. (2015) provides insight into the physiological processes controlling peroxisome-chloroplast interaction (photosynthesis dependent), but they did not determine the effective baseline force required to move peroxisomes that were not next to chloroplasts under control or altered environmental conditions. Comparisons between the relative forces required to move peroxisomes next to chloroplasts versus those that are not next to chloroplasts are critical in understanding and probing the physical interaction between the two organelles, the hypothesis being that tethering would increase the force required to move peroxisomes compared with organelles that are not tethered. Since peroxisomes have diverse biochemical roles that affect a wide range of physiological processes throughout the plant life cycle (Hu et al., 2012), an understanding of if and how peroxisomes may interact with other subcellular structures is likely to be an important consideration for efficient peroxisome function.

Peroxisomes are highly pleomorphic, dynamic organelles bounded by a single membrane (Hu et al., 2012), whose movement is driven by acto-myosin-dependent processes (Jedd and Chua, 2002; Mano et al., 2002; Mathur et al., 2002; Avisar et al., 2008; Sparkes et al., 2008). Tubular emanations termed peroxules (Scott et al., 2007) can extend from the main peroxisome body, yet it is unclear what function they may play. Formation is quite frequent in hypocotyl cells (Cutler et al., 2000; Mano et al., 2002; Sinclair et al., 2009), can occur around chloroplasts in cotyledonary leaf pavement cells (Sinclair et al., 2009), and is not always from the trailing edge of the peroxisome (Sinclair et al., 2009). Exogenous addition of hydroxyl reactive oxygen species (ROS), or exposure to UV light, induces peroxule formation (Sinclair et al., 2009). It has been suggested that they represent an increased surface area for increased biochemical function or might represent a morphological precursor for peroxisome division (Jedd and Chua, 2002). Based on subcellular coalignment, a retro-flow model for the potential exchange of luminal content between the endoplasmic reticulum (ER) and peroxisome through the peroxule has been suggested (Sinclair et al., 2009; Barton et al., 2013). However, these studies, as with many others, interpret the close association between organelles to indicate physical connectivity between organelles, whereas, in fact, in highly vacuolated leaf epidermal cells, organelles can be closely packed within the cytoplasm due to mere spatial constrictions generated through the large central vacuole. This is further complicated by the highly motile, and seemingly stochastic, nature of acto-myosin-driven organelle movement, resulting in frequent apparent organelle collisions that may not reflect a functional requirement for organelle interaction.

Optical trapping provides a highly specific and sensitive means to measure physical connectivity between organelles. By focusing an infrared beam, it allows the user to trap objects that have a significantly different refractive index from the surrounding medium. Upon trapping, the user can then move the trapped object relative to its original position to gain an understanding of whether the movement affects the position and motion of other structures (such as other organelles) that may be physically attached to the trapped organelle. For example, unlike the ER, Golgi bodies are amenable to trapping. By trapping and micromanipulating (i.e. precisely moving) the Golgi, a physical association between the ER and the Golgi was determined in a qualitative manner (Sparkes et al., 2009b). Here, we

have developed a system to generate quantitative measures for organelle interaction by standardizing and automating how far we move the trapped organelle (which we call the translation step) at a defined speed and assessing how trapping efficiency alters in response to the power of the laser trap itself. By using these parameters, we can then model the forces imparted on the organelle, providing further insight into the tethering processes.

Our results indicate that peroxisomes are amenable to being trapped, that they physically interact with chloroplasts in leaf epidermal cells, and, surprisingly, that peroxisomes are also tethered to other unknown structures within the cell. This approach highlights that organelle interactions within plant cells are not random but regulated through tethering. In addition, we provide a novel role for peroxules and a simple biophysical model to describe peroxisome motion during the trapping process.

RESULTS

Peroxisome Association with Chloroplasts Is Specific

For organelles to interact, they must move and physically sit or reside next to one another in a coordinated manner. To determine how peroxisomes move relative to chloroplasts, we observed peroxisomes, chloroplasts, and Golgi bodies within the same tobacco (*Nicotiana tabacum*) leaf epidermal cell and assessed how long either peroxisomes or Golgi bodies resided next to chloroplasts. As organelles are physically constrained by the large central vacuole and can be pushed together, the Golgi bodies were monitored, as they are not functionally related to chloroplasts and so act as an inherent control. We observed that the average residency time of peroxisomes was significantly higher than that of Golgi bodies on chloroplasts: 1.46 ± 0.35 min (n = 17) and 0.42 ± 0.05 min (n = 51), respectively (Student's t test $P < 0.001$; Supplemental Movie S1). Due to these observations, and the functional connectivity through the photorespiratory pathway, we investigated whether peroxisomes interact physically with chloroplasts in vivo.

Peroxisomes Are Associated with Chloroplasts in an Actin-Independent Manner

In a motile system, it is difficult to discriminate between physical tethering processes between two organelles from acto-myosin-driven events. Therefore, we assessed whether interaction characteristics were actin dependent in the first instance. Note that the concentration of latrunculin b used is sufficient to depolymerize actin and cause the cessation of organelle movement (Sparkes et al., 2008, 2009a).

The average percentage of chloroplasts with a juxtaposed peroxisome in the presence or absence of actin (latrunculin b treated) was not significantly different from one another: 22% ± 5% and 23% ± 3%, respectively (Student's t test $P > 0.8$; data taken from 20 images covering a 0.4-mm^2 leaf epidermal area). Using optical tweezers, we then tested whether these results indicated a peroxisome-chloroplast tethering mechanism in both motile and nonmotile (latrunculin b-treated) samples. By trapping and subsequently moving the peroxisome within the cell (Fig. 1, A–D), we observed that, upon turning the trap off, the peroxisome recoiled back toward its place of origin irrespective of chloroplast presence (Supplemental Movie S2, B–D). To our knowledge, this process has not been observed previously using other techniques. On several occasions, peroxules were observed from the trailing edge of the peroxisome (Supplemental Movie S2, B and D). Upon actin depolymerization, trapped peroxisomes displayed similar characteristics: peroxule formation

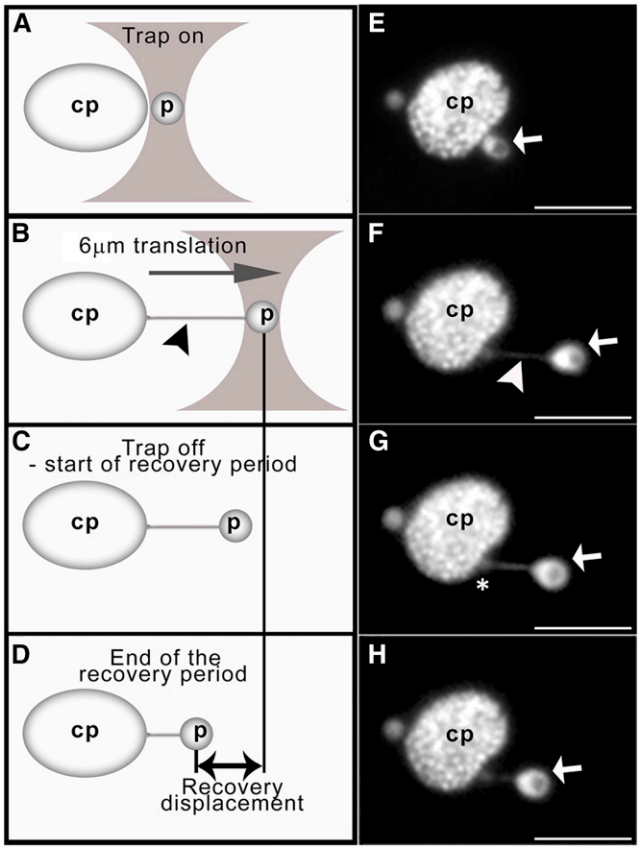

Figure 1. Optical trapping and movement of peroxisomes away from chloroplasts in tobacco leaf epidermal cells. Schematic representations of the trapping procedure (A–D) and corresponding micrographs (E–H) are shown. Upon turning the trap on (A and E) and moving the stage 6 μm at a set speed (B and F; referred to as the translation period), the trapped peroxisome (p; white arrows) is pulled away from the cp and a peroxule (arrowheads) is formed. Upon turning the trap off (C and G), the peroxisome recoils backs toward its original position next to the chloroplast (D and H). Peroxisome displacement during the recovery period (referred to as recovery displacement) is measured (double-headed arrow). The asterisk denotes the tip of the peroxule. Bars = 6 μm.

and peroxisome recoil upon turning the trap off (Fig. 1, E–H; Supplemental Movie S3, A and B). These results indicated that peroxisomes are tethered to chloroplasts and unknown structures in the cell and that peroxules may represent the site of tethering.

To test the hypothesis that peroxisomes are tethered to chloroplasts, we set about quantifying whether the average laser power required to trap and move peroxisomes was dependent on chloroplast positioning and/or actin. The rationale here is that trapping efficiency and movement are dependent on optical trap strength, where tethering, which acts as an opposing force, would impede the movement of the trapped organelle, causing it to escape the trap. Trapping refers to an organelle that can be trapped and remains in the trap over the 6-μm translation distance (Fig. 1). Of the 50 organelles from independent cells that underwent the trapping routine (which constituted five samples of 10 organelles), there was a clear trend that increasing optical laser power (from 24 to 50 mW) resulted in an increase in the number of trapped peroxisomes (20%–38% increase) irrespective of actin or chloroplast association. However, peroxisomes that were next to chloroplasts were harder to trap. Significantly fewer chloroplast-associated (cp) peroxisomes were trapped when compared with non-chloroplast-associated (noncp) peroxisomes under either motile or immotile (latrunculin b-treated) conditions at a given laser power; 50-mW optical trapping laser power resulted in average trapping of 38% $\pm$ 2% cp peroxisomes and 56% $\pm$ 7% noncp peroxisomes in the motile system and 36% $\pm$ 4% cp peroxisomes and 70% $\pm$ 4% noncp peroxisomes in the immotile system (Student's t test $P < 0.05$, comparing cp with noncp peroxisomes under a given condition). These results indicate that peroxisomes are tethered to chloroplasts and that this phenomenon is independent of actin. The trapping efficiency of noncp peroxisomes in the motile system compared with the immotile system was significantly reduced (Student's t test $P < 0.15$) and could be due to a number of reasons: trapped peroxisome being knocked out of the trap by passing organelles, docking the peroxisome onto actin filaments during the translation, or moving a trapped organelle into a cytoplasmic stream (Supplemental Movie S2).

Peroxisome tethering can also be quantified by monitoring the recoil of the peroxisome back toward its origin after turning the trap off (Fig. 1; termed recovery displacement). However, inherent difficulties of organelles escaping the trap and responding to the acto-myosin-driven elements after turning the trap off reduced the number of organelles that could be assessed in this manner; for cp motile and cp/noncp nonmotile systems (latrunculin b treated), between 66% and 84% were measurable, compared with 21% for the noncp motile system. Observations of the small number of organelles that showed recoil back toward the trap origin (recovery displacement; Fig. 1), rather than movement in the opposite direction in the motile system, indicated that recoil was significantly larger for cp compared with noncp systems in both motile and nonmotile conditions: for the motile system, cp recovery displacement was 3.92 $\pm$ 0.36 μm ($n = 16$) compared with noncp recovery displacement of 2.5 $\pm$ 0.29 μm ($n = 6$; $P < 0.007$); for the nonmotile system, cp recovery displacement was 3.65 $\pm$ 0.45 μm ($n = 14$) compared with noncp recovery displacement of 1.22 $\pm$ 0.2 μm ($n = 23$; $P < 0.001$). All data were taken using 50-mW trapping laser power with a 5.3-s recovery period.

Quantifying the Peroxisome-Chloroplast Tethering Process: A Novel Role for Peroxules

The above observations clearly indicate that peroxisomes are tethered to chloroplasts and that this phenomenon is independent of actin. To further characterize the effects of tethering, the opposing forces generated by the acto-myosin component were removed from the system (latrunculin b treatment). Here, we assessed (1) the relationship between peroxisome behavior in the trap and trapping laser power over a larger range of laser powers and (2) the behavior of displaced peroxisomes after turning the trap off (Figs. 1 and 2). All of these observations were carried out under latrunculin b treatment, so that any interactions are due to tethering and not the acto-myosin system.

Peroxisomes were either trapped, not trapped, or escaped the trap during translation (Fig. 2C; Supplemental Movie S3, C–E). As expected, the trapping laser power correlated with the observed percentage of trapping for both cp and noncp peroxisomes (Fig. 2, A and B). However, at laser powers of 37 mW and above, there was a significant difference between the trapping of cp and noncp peroxisomes, with cp peroxisomes escaping the trap more readily and noncp peroxisomes being trapped and remaining in the trap over the 6-μm translation (Fig. 2; Supplemental Fig. S1). Taken together, this is indicative of more force being required to trap and move peroxisomes away from chloroplasts. Additionally, upon turning the trap off, cp trapped peroxisomes underwent a significantly larger recovery displacement (i.e. recoil; Fig. 1D) than noncp trapped organelles: cp recovery displacement was 4.39 $\pm$ 0.17 μm ($n = 94$) and noncp recovery displacement was 2.93 $\pm$ 0.17 μm ($n = 91$) using a laser power of 37 mW, which has a Student's t test value of $P < 0.001$. This proves that peroxisomes are tethered to chloroplasts in vivo in tobacco leaf epidermal cells. The above data were generated under a long recovery period (21.5 s rather than 5.3 s) to allow organelles to reach their equilibrium position, which improves the accuracy of the force determination discussed later.

Peroxule formation can occur upon exposure to the trapping laser prior to and during the translation; however, the frequency of formation is independent of the power of the optical trapping laser, indicating that formation is not solely due to exposure to the trapping laser (Supplemental Table S1). Interestingly, both cp (38%; $n = 170$) and noncp (37%; $n = 183$) peroxisomes had a similar propensity to form peroxules, but the

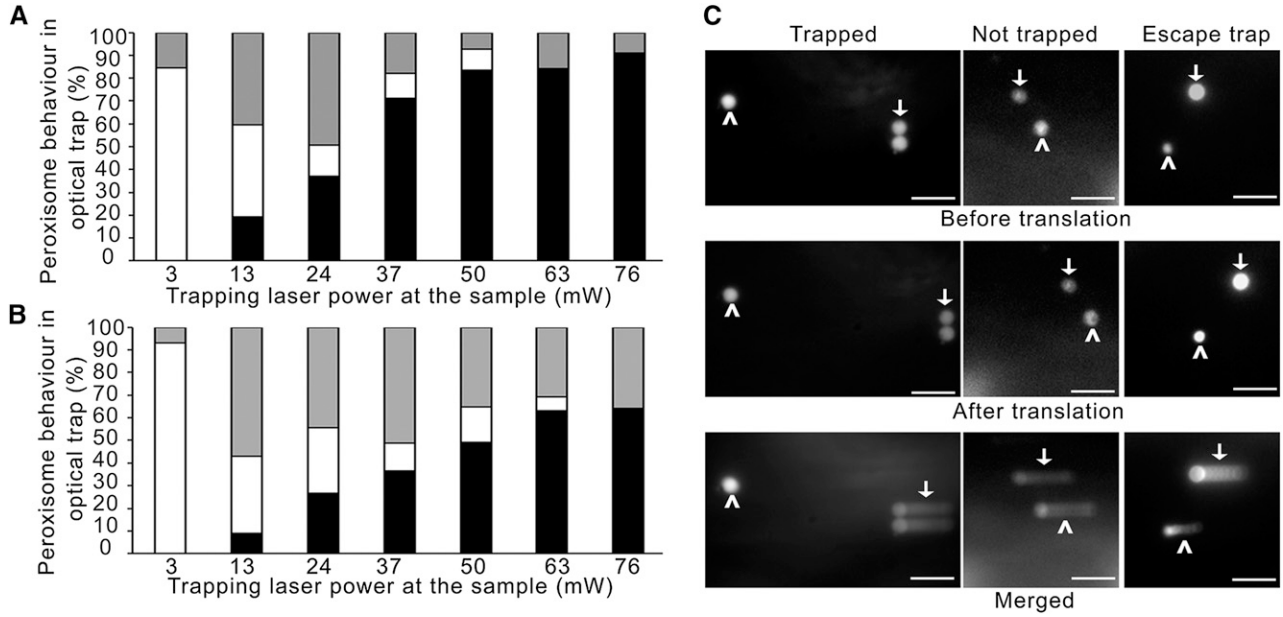

Figure 2. Higher optical trapping laser power is required to trap and move peroxisomes away from chloroplasts. The noncp (A) and cp (B) peroxisomes underwent the optical trapping protocol using various trapping laser powers, and their trapping characteristics were scored: peroxisomes that remained in the trap over the 6-μm translation (black bars), were unable to be trapped (white bars), or escaped the trap during the translation (gray bars). Percentages displayed are based on weighted means from a set of independent experiments. Supplemental Figure S1 compares cp with noncp peroxisomes for all three trapping categories and indicates significant differences between peroxisomes that are trapped or that escape from the trap for cp versus noncp samples. The relationship between optical laser trap power and peroxule formation is given in Supplemental Table S1. C shows still images from Supplemental Movie S3, C to E, representing before and after translation events for peroxisomes that are trapped, not trapped, or escape the trap during the translation event (arrowhead). Note that peroxisomes not subjected to trapping in the same cell are shown for comparison (arrows). The translation event is based on the movement of the stage and not the trap. Composite images of frames captured during the translation event show that the trapped peroxisome does not appear to move whereas organelles that escape the trap or are not trapped result in comet-like tails (merged). Bars = 6 μm.

relative percentages between formation in response to exposure to the optical trap versus translation differed (Supplemental Table S1). It is unclear why more peroxules would form in the absence of chloroplast positioning prior to translation (2.9% compared with 12%), but we speculate that formation may occur in response to stress that is ameliorated by the antioxidant properties of the chloroplast (Asada, 2006; Sinclair et al., 2009) or that noncp peroxisomes are tethered to structures whose positioning alters in response to trapping the peroxisome.

During peroxisome translation, peroxule formation is more frequent in cp versus noncp peroxisomes (28.2% compared with 15.3%; Supplemental Table S1), correlative with peroxules being the visible manifestation of the tether to chloroplasts. The tip (point of origin; Fig. 1G, asterisk) of peroxules moved less during the translation process in cp versus noncp conditions, indicative of an anchored tether: cp value was 1.85 $\pm$ 0.3 μm (n = 37) and noncp value was 2.35 $\pm$ 0.2 μm (n = 46). In comparison, during the recovery period, peroxule tip displacement was much smaller, with cp and noncp values being similar: cp value was 0.89 $\pm$ 0.2 μm and noncp value was 1.13 $\pm$ 0.1 μm. If the base of the tether (i.e. peroxule tip; Fig 1G, asterisk) is anchored, one would expect a higher level of peroxisome movement (i.e. recoil) during the recovery period to correspond with a lower level of peroxule tip movement during the translation; unlike noncp samples, there is a cluster of cp samples indicative of such behavior, suggesting strongly anchored tether bases (Fig. 3).

Biophysical Modeling of Peroxisome Recoil Indicates Differences in Relative Forces for Peroxisome Interactions

Since both cp and noncp peroxisomes exhibit different trapping (Fig. 2) and recovery (Fig. 3) behaviors, we sought to understand the forces involved in this process; specifically, is it only the recoil distance that changes, or are there changes in the tether properties between cp and noncp peroxisomes? To allow us to distinguish between tether properties and changes in recoil distance, we used a simple viscously damped spring model to estimate the tether stiffness (i.e. spring constant) and tether tension forces (i.e. initial recovery force) involved in the recovery process (Fig. 4; Supplemental Note S1; Supplemental Figs. 2–4). This first approximation indicates that tether stiffness values are similar for noncp and cp samples (Fig. 4, B and C)

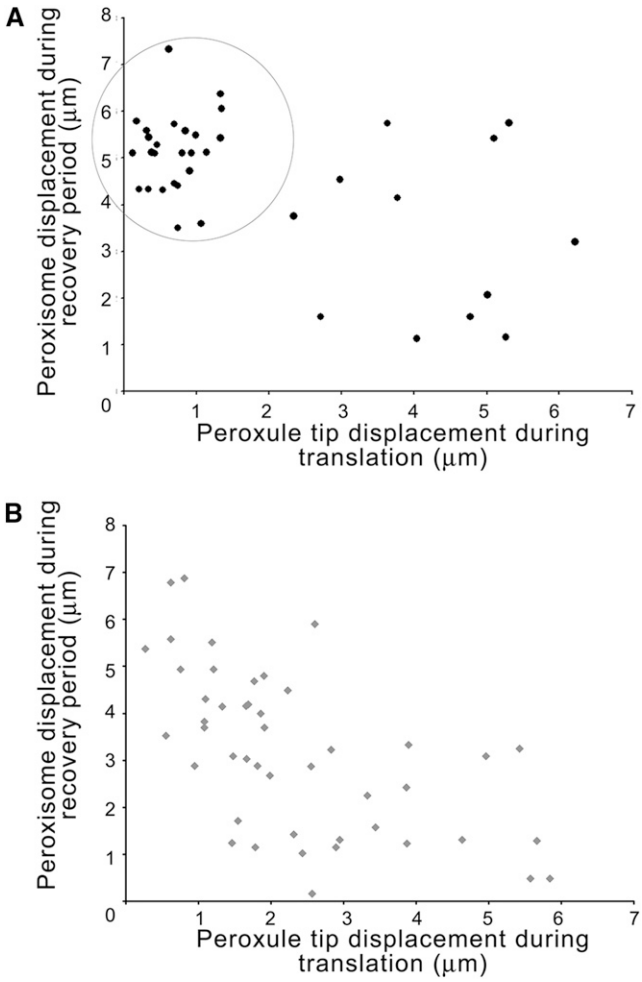

Figure 3. Correlation between peroxisome displacement during the recovery period and peroxule tip displacement during translation indicates anchored tethering between chloroplasts and peroxisomes. Peroxule tip displacement during the translation period was plotted against the peroxisome displacement during the recovery period for cp (A; $n = 37$) and noncp (B; $n = 46$) peroxisomes. Peroxisomes were trapped with 37-mW optical trap laser power followed by a 21.5-s recovery period. The behavior of cp samples is indicative of anchored tethers, where the peroxule tip represents the base of the tether: small peroxule tip displacement combined with large peroxisome recovery displacement (circle). Note that the sample sizes are different from those in Supplemental Table S1, as displacement could only be measured if the peroxule was observable for the entire period.

and that differences in the recovery forces are solely due to the more rigid anchoring of cp peroxisome tethers, which leads to greater tether extension and, subsequently, greater recovery displacement and initial recovery forces (Fig. 4). In other words, the biological structure that forms the tether between cp and noncp peroxisomes behaves in a similar manner (i.e. similar stiffness), but the base of the tether (i.e. anchor point) moves less for cp peroxisomes, thus generating more tension during translation and resulting in greater recoil. Here, noncp peroxisomes are tethered to a structure that has greater mobility than chloroplasts during the trapping routine, so that upon moving noncp peroxisomes, the tethered structure is also able to move to a certain extent, resulting in lower tension buildup during the translation process. As we cannot independently estimate cytoplasmic viscosity in our system, this approach can only be used to determine relative differences in forces between cp and noncp peroxisomes. However, using a reasonable value of 0.06 Pa s (Scherp and Hasenstein, 2007) gives a tether stiffness of approximately 1 pN μm^{-1} and initial recovery forces of approximately 1 to 4 pN (median values from Fig. 4).

DISCUSSION

By using optical tweezers, we clearly show that peroxisomes can be tethered to chloroplasts and that relative differences in tethering strength highlight additional subcellular interactions. Moreover, these tethers can be observed in several instances as peroxules (Supplemental Movies S2 and S3). Such tethers are not solely restricted to chloroplast interaction but are also prevalent on noncp peroxisomes (Supplemental Movies S2 and S3). In the latter case, the tether interaction is either unstable or the structure it is tethered to is more readily motile, accounting for the movement of the peroxule tip base during translation. The mechanism of peroxule formation and extension is unclear, but the rapid rate of extension makes de novo synthesis unlikely. Alternatives could be that the bounding membrane itself is deformable or that peroxules are tightly coiled around the peroxisome and indistinguishable from the fluorescence signal arising from the lumen of the main peroxisome body. It is unclear if the connectivity between peroxisomes and chloroplasts is direct or indirect, as positioning could be mediated through interaction with the ER. The ER forms a basket around the chloroplasts (Schattat et al., 2011), and in vitro optical trapping data suggested a chloroplast-ER connection in Arabidopsis and pea (*Pisum sativum*) leaf cells (Andersson et al., 2007). The peroxisomal membrane protein PEX3p has been implicated in acting as a direct tether between the ER and peroxisomes in *Saccharomyces cerevisiae* (Knoblach et al., 2013). However, the complex biogenetic link between peroxisomes and the ER has been, and continues to be, debated within the community (Hu et al., 2012). Our previous observations of ER responses upon trapping and moving the Golgi highlight that a large percentage of the ER is freely mobile; however, chloroplast-ER interactions were not investigated (Sparkes et al., 2009b). Therefore, if chloroplast-peroxisome connectivity is mediated by an ER bridge, then perhaps the ER is highly constrained around chloroplasts, which could lead to greater recoil of trapped cp peroxisomes compared with noncp cases. This is an area of future study requiring further development of the imaging system. Using the approaches developed here, future studies will enable the molecular and physiological consequences of peroxisome-organelle interaction to be

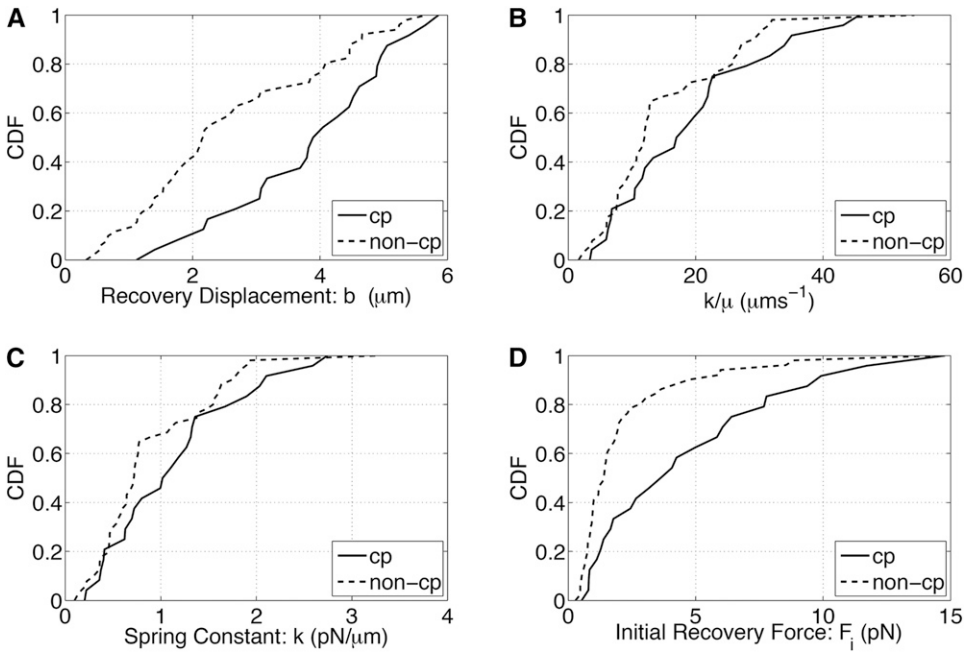

Figure 4. Cumulative distribution functions (CDF) of model parameters for cp and noncp peroxisomes. Recovery displacement b is larger for cp than noncp peroxisomes (A), whereas k/μ values, indicative of the tether stiffness, are broadly similar (B). Also shown are the derived spring constants (C) and initial recovery forces (D) calculated assuming a viscosity of 0.06 Pa s for the cytoplasm. Values are derived using the spring model described in Supplemental Figures S2 to S4.

studied and could also be used to study the formation of membrane extensions.

Interactions between organelles are likely required for communication and transport. Examples in yeast and mammals infer a requirement for lipid and calcium exchange (Prinz 2014). In plants, reports for ER-Golgi (Sparkes et al., 2009b), nucleus-plastid (Higa et al., 2014), ER-chloroplast (Andersson et al., 2007; Mehrshahi et al., 2013), and peroxisome-oil body (Thazar-Poulot et al., 2015) interactions have been made, along with a recent report from Oikawa et al. (2015) suggesting a chloroplast-peroxisome interaction in Arabidopsis mesophyll cells. This study, along with previous reports, indicates that peroxisomes undergo light-dependent morphological changes (Desai and Hu, 2008; Oikawa et al., 2015). Furthermore, by effectively inducing a localized intracellular shock wave, Oikawa et al. (2015) suggested light- and photosynthesis-dependent connections between peroxisomes and chloroplasts. Here, using a complementary approach, we trap individual peroxisomes in tobacco leaf epidermal cells and additionally compare the responses between cp and noncp peroxisomes. Our results provide a clear indication of the interaction of peroxisomes with chloroplasts and other unknown structures, and we provide a biophysical model for the forces involved in the tethering process. We have also visualized the tethering process through peroxule production, observations that were not made in the work of Oikawa et al. (2015) and, therefore, suggest a novel role for peroxules in maintaining physical connectivity between peroxisomes and the structure(s) to which it is tethered. The two techniques suggest forces for the peroxisome-chloroplast interaction, but by the very nature of the techniques the forces relate to different biological aspects of the interaction. Oikawa et al. (2015) modeled the force required to push the two organelles apart (23–61 fN nm^{-2}), whereas here we model the forces imparted on the organelle after they have been separated. It is important to note that the speed used to separate the organelles using optical tweezers is within the range of reported peroxisome speeds in an unperturbed system (Sparkes et al., 2008), and so cytoplasmic viscosity will affect interactions in a way that reflects the native motile system. However the force imparted on peroxisomes using the focused femtosecond laser technique was reported to be so large that the effects of cytoplasmic viscosity would not hinder free peroxisome motion and, therefore, are negligible in their system. We do not suggest a precise force for trapping and moving the organelle (as viscosity values are currently unknown for the system) and so compare the trapping profiles of cp and noncp peroxisomes in response to the trapping laser power. Therefore, both systems provide different force components and have different strengths and weaknesses in assessing the peroxisome-chloroplast interaction. Furthermore, the basic spring model provides a baseline for interactions and will be useful in testing how effective tension and stiffness change under altered environmental conditions that may regulate the interaction between peroxisomes and chloroplasts. For example, as photorespiration and photosynthesis may affect interaction, does the rate of recoil of a trapped peroxisome change, indicating a tighter tethering process between peroxisomes and chloroplasts or other structures within the cell, and does this altered response affect tether stiffness rather than tension?

Several organelles in plant cells produce tubular emanations; stromules, matrixules, and peroxules extend

from chloroplasts, mitochondria, and peroxisomes, respectively (Scott et al., 2007; Mathur et al., 2012; Hanson and Sattarzadeh, 2013). Mapping stromule dynamics and the movement of protein and small molecules lend support to a role in communication. However, contradictory data from different groups on the molecular exchange between stromules make this an interesting and contentious area of research (Hanson and Sattarzadeh, 2013; Mathur et al., 2013). Here, our results suggest a similar role in communication, and we propose that tubular emanations are a consequence of organelles attempting to maintain connections in the highly dynamic intracellular environment. Peroxule formation occurs in response to hydroxyl ROS with a concomitant reduction in peroxisome speed (Sinclair et al., 2009). This could be interpreted as a response to maintain connections between peroxisomes and another organelle whose motility has not been affected or has been increased during this treatment, effectively increasing the spatial separation between the two organelles. While the biophysical model provided herein reveals pN force measurements imparted on the organelle during the recovery process, it also gives an indication of the force required to pull the organelle micron distances. Here, the motor force to separate organelles is expected to be the same or greater than the force required for the organelles to be pulled back toward their resting position (i.e. referred to as the restorative force in the biophysical model). This approach could determine how motor regulation is controlled in order to maintain peroxisome movement under conditions where interaction with chloroplasts is up-regulated and/or down-regulated.

Organelle movement plays important roles in growth, development, and in response to (a)biotic stresses (for refs., see Madison and Nebenführ, 2013; Buchnik et al., 2015). In a wider context, the results presented herein allow us to start to bridge the interface between organelle movement and interaction and the forces involved in these processes. While future studies are required to validate the force measurements with known cellular viscosities, in broader terms, these studies demonstrate that interactions between organelles such as peroxisomes and chloroplasts in plant cells are not random but are controlled through tethering mechanisms that can be quantified using optical tweezers. The regulation of organelle interaction/association will be controlled by motor-driven movement to position organelles next to one another to allow tethering processes to occur. Therefore, the force balance between these two processes needs to be viewed in conjunction to describe organelle motion and positioning. Organelle interactions in plants could be required for communication, so future studies pinpointing the tethering and motor components could provide a novel way in which to control subcellular communication.

An interdisciplinary approach will be needed to fully characterize the molecular and physiological role(s) of peroxisome-chloroplast interactions and interactions with other unknown organelles that could include lipid bodies. Current evidence points toward photosynthesis-dependent processes and a role for PEX10 in peroxisome-chloroplast interactions (Schumann et al., 2007; Prestele et al., 2010; Oikawa et al., 2015). It will also be interesting to assess what role ROS signaling may play in these interactions (Sandalio and Romero-Puertas, 2015) and whether the exchange of additional small molecules such as indole-3-acetic acid and jasmonic acid may be facilitated by organelle interaction. Future genetic screens and proteomic approaches will pinpoint the complex of proteins necessary for interaction. The essential domains required for tethering will be mapped using biophysical means, such as optical tweezers, to quantify the effects on peroxisome-chloroplast/organelle interaction. Ultimately, the analysis of resulting lines deficient in the tethering process will provide molecular, biochemical, and physiological evidence for the role of peroxisome-chloroplast/organelle interaction.

MATERIALS AND METHODS

Plant Material and Sample Generation

Tobacco (*Nicotiana tabacum*) plants were grown and transiently transformed according to Sparkes et al. (2006). GFP-SKL (Sparkes et al., 2003), YFPSKL (Mathur et al., 2002), and StCFP (Brandizzi et al., 2002) constructs were infiltrated at 0.04 optical density. Leaf samples (approximately 5 mm^2) were taken from plants after 3 to 4 d of expression and incubated in 25 μM latrunculin b for 60 min prior to imaging.

Confocal Imaging and Determination of Organelle Association and Residency Time with Chloroplasts

Triple imaging of peroxisomes (YFPSKL), Golgi (StCFP), and chloroplasts (autofluorescence) in live tobacco epidermal pavement cells was done using multitracking in-line switching mode on a Zeiss LSM510 Meta confocal microscope. Cyan fluorescent protein was excited with a 458-nm argon laser and yellow fluorescent protein/chloroplast autofluorescence with a 514-nm laser, and their emissions were passed through an HFT 458/514 main dichroic beam splitter and NFT 490 and NFT 595 secondary dichroic beam splitters and detected using 470- to 500-nm, 530- to 600-nm, and 647- to 690-nm filters, respectively. All imaging was carried out using a 63× 1.4 numerical aperture (NA) oil-immersion objective with a scan speed of 1.94 frames per second. Peroxisomes/Golgi that were up to 1 μm from the chloroplasts (as monitored by the autofluorescent signal) were categorized as residing next to chloroplasts. The residency times of peroxisomes and Golgi on chloroplasts were analyzed manually. Only those that resided next to (and could move laterally over the surface of) the chloroplast for more than 3 s were included in the statistical analysis.

Dual imaging of peroxisomes (GFPSKL) and chloroplasts (autofluorescence) was carried out using multitracking in line-switching mode on a Zeiss LSM510 Meta confocal microscope. GFP was excited with a 488-nm argon laser and autofluorescence with a 514-nm laser, and their emissions were passed through an HFT 488/543 main dichroic beam splitter and NFT 515 and NFT 545 secondary dichroic beam splitters and detected using 505- to 530-nm and 636- to 690-nm filters, respectively. All imaging was carried out using a 63× 1.4 NA oil-immersion objective. Twenty single scans of a 143- × 143-μm area were taken, and the number of chloroplasts with a juxtaposed peroxisome in each image was counted.

Optical Trapping Setup and Data Generation

Optical trapping was performed using a cw 1090 nm laser (SPI) focused using a 100×, oil-immersion, NA 1.49 TIRF objective lens (Nikon). Here, we assume that the effective NA of the objective lens for optical trapping approaches a value of 1. The assumption is based upon a comparison of escape force measurements made on 1-μm-diameter polystyrene beads to theoretical values calculated using an optical tweezers computational toolbox (Nieminen et al.,

2007). TIRF objectives are not commonly used for optical tweezers. Mahamdeh et al. (2011) also indicate that spherical aberrations arising from trapping in aqueous medium will reduce the effective NA.

TIRF used an excitation laser with 473-nm wavelength (Becker and Hickl) with a maximum output power of 5 mW, coupled by an optical fiber to a Nikon TIRF adapter system and attenuated by neutral density filters (two and/or eight, dependent on the level of GFP-SKL expression). Emitted fluorescent light was filtered using a long-pass filter for wavelength transmission above 505 nm and imaged using an electron-multiplier CCD (Andor Ixon EMCCD). This allowed visualization of the excited GFP-SKL probe and detection of chloroplast autofluorescence. Note that while the TIRF technique was employed to give significant improvement of signal to noise, it is also likely that we are operating in a highly inclined illumination.

Custom LabVIEW software (National Instruments) was used to control the EMCCD camera (Andor Ixon), microscope stage (Marshauser), and a shutter, which blocked the laser beam used for trapping. A LabVIEW interface was used to synchronize the timing of peroxisome capture, stage translation, and peroxisome release over 110- or 229-frame videos; peroxisomes were monitored for 10 frames prior to trap activation, 40 frames upon trap activation prior to movement, 10 frames for the 6-μm translation, 10 frames after the translation, and 40 or 159 frames after the trap was deactivated (relating to 5.3- or 21.5-s recovery periods, respectively). Stage translation was measured to be 5.74 μm in 1 s, with the EMCCD cycle time of 0.135 s giving approximately 7.5 frames per second. The video sequences were stored as 16-bit stacked tagged image file format files for subsequent analysis of peroxisome behavior. Note that the data sets generated for Figure 2 are combinations of the above trapping routine and an earlier version where trap shuttering was manually controlled over a 70-frame video.

The minimal force (i.e. the escape force) required to trap peroxisomes, in a noncp environment, was measured by application of a viscous drag force (Supplemental Fig. S2). The laser trap strength and viscous properties were investigated using a set of controlled experiments where the stage velocity was varied. For each stage velocity, the laser power required to keep 50% of the captured peroxisomes in the optical trap was determined over a fixed 6-μm translation distance (Supplemental Fig. S2). The fluorescent organelles were observed under TIRF illumination. Due to variability in peroxisome diameter, it was necessary to measure 30 to 80 peroxisomes at each stage velocity to obtain a representative laser power. Thus, the reported laser power is for an average peroxisome (with plotted error bars indicating SE uncertainty in laser power). The viscous drag force for each stage velocity was calculated using Stokes' law with an assumed viscosity value of 0.06 Pa s (Scherp and Hasenstein, 2007) and the average measured peroxisome diameter. Error bars for viscous drag force calculations used the SE variation of peroxisome diameter. As a control, the same procedure was applied to 1-μm-diameter polystyrene beads in water (0.00089 Pa s).

Analysis of Optical Trapping Data

Trapping data from each repetition were normalized against differences in sample size to determine the percentages of peroxisomes that were either trapped, not trapped, or escaped the trap per leaf sample. The weighted mean values were taken of these percentages for whole data sets and plotted. Between 36 and 62 peroxisomes underwent the trapping protocol at any given laser trapping power, resulting in $n = 338$ for cp and $n = 381$ for noncp total sample sizes. These totals represent between five and nine repetitions, where each repetition is from one leaf sample taken from six to nine independent plants. Trapping was only attempted once per peroxisome, and repeated trapping of the same peroxisome was not undertaken.

Displacement values for peroxisome and peroxule dynamics were determined using ImageJ.

In order to gather statistically significant peroxisome motion data, we developed a customized detection and tracking algorithm using a combination of python (scipy) and custom-written scripts and algorithms. The data were first filtered using the Laplace-of-Gaussian scale-space method (Lindeberg, 1994) to selectively filter for objects in a given size range. Next, robust image statistics-based thresholding (median absolute deviation) selected only salient objects in the resulting filtered data as outlined by Murtagh and Starck (2000). Object tracking was performed using a global nearest neighbors point registration approach, implemented as a modified version of the Jonker-Volgenant linear assignment problem algorithm, altered to allow rectangular cost matrices and cost cutoffs. In addition, subpixel peroxisome positions were calculated using a filtered intensity weighted centroid function. Tracking validation was performed by manual verification. The resulting trajectories were then analyzed to determine the peroxisome motion between the moment that the optical trap was disengaged and the end of the recovery period.

Force calculations are described in the spring model (Supplemental Note S1).

Supplemental Data

The following supplemental materials are available.

Supplemental Figure S1. Relationship between cp and noncp peroxisomal behavior in the optical trap.

Supplemental Figure S2. Laser power required for trapping peroxisomes and polystyrene beads at different stage velocities.

Supplemental Figure S3. Spring model definition.

Supplemental Figure S4. Example fits to the data using the simple spring model.

Supplemental Table S1. Relationship between optical laser trap power and peroxule formation characteristics from cp and noncp peroxisomes.

Supplemental Movie S1. Peroxisome association with chloroplasts.

Supplemental Movie S2. Peroxisomes can be trapped and moved laterally within tobacco leaf epidermal cells.

Supplemental Movie S3. Peroxisome behavior in the optical trap under actin depolymerization.

Supplemental Note S1. Spring model of peroxisome motion.

ACKNOWLEDGMENTS

We thank Anne Kearns and Ian Leaves for technical assistance with growing the tobacco plants required for the experiments, members of the plant cell biology group at Oxford Brookes University for help with experimental logistics, and Jaideep Mathur and Chris Hawes for the YFPSKL and StCFP, respectively.

Received September 28, 2015; accepted October 24, 2015; published October 30, 2015.

LITERATURE CITED

Andersson MX, Goksör M, Sandelius AS (2007) Optical manipulation reveals strong attracting forces at membrane contact sites between endoplasmic reticulum and chloroplasts. J Biol Chem **282:** 1170–1174

Asada K (2006) Production and scavenging of reactive oxygen species in chloroplasts and their functions. Plant Physiol **141:** 391–396

Avisar D, Prokhnevsky AI, Makarova KS, Koonin EV, Dolja VV (2008) Myosin XI-K is required for rapid trafficking of Golgi stacks, peroxisomes, and mitochondria in leaf cells of *Nicotiana benthamiana*. Plant Physiol **146:** 1098–1108

Barton K, Mathur N, Mathur J (2013) Simultaneous live-imaging of peroxisomes and the ER in plant cells suggests contiguity but no luminal continuity between the two organelles. Front Physiol **4:** 196

Brandizzi F, Snapp EL, Roberts AG, Lippincott-Schwartz J, Hawes C (2002) Membrane protein transport between the endoplasmic reticulum and the Golgi in tobacco leaves is energy dependent but cytoskeleton independent: evidence from selective photobleaching. Plant Cell **14:** 1293–1309

Buchnik L, Abu-Abied M, Sadot E (2015) Role of plant myosins in motile organelles: is a direct interaction required? J Integr Plant Biol **57:** 23–30

Bussell JD, Behrens C, Ecke W, Eubel H (2013) Arabidopsis peroxisome proteomics. Front Plant Sci **4:** 101

Cutler SR, Ehrhardt DW, Griffitts JS, Somerville CR (2000) Random GFP: cDNA fusions enable visualization of subcellular structures in cells of Arabidopsis at a high frequency. Proc Natl Acad Sci USA **97:** 3718–3723

Desai M, Hu J (2008) Light induces peroxisome proliferation in Arabidopsis seedlings through the photoreceptor phytochrome A, the transcription factor HY5 HOMOLOG, and the peroxisomal protein PEROXIN11b. Plant Physiol **146:** 1117–1127

Frederick SE, Newcomb EH (1969) Microbody-like organelles in leaf cells. Science **163:** 1353–1355

Hammer JA III, Sellers JR (2012) Walking to work: roles for class V myosins as cargo transporters. Nat Rev Mol Cell Biol **13:** 13–26

Hanson MR, Sattarzadeh A (2013) Trafficking of proteins through plastid stromules. Plant Cell **25:** 2774–2782

Higa T, Suetsugu N, Kong SG, Wada M (2014) Actin-dependent plastid movement is required for motive force generation in directional nuclear movement in plants. Proc Natl Acad Sci USA **111:** 4327–4331

Hu J, Baker A, Bartel B, Linka N, Mullen RT, Reumann S, Zolman BK (2012) Plant peroxisomes: biogenesis and function. Plant Cell **24:** 2279–2303

Jedd G, Chua NH (2002) Visualization of peroxisomes in living plant cells reveals acto-myosin-dependent cytoplasmic streaming and peroxisome budding. Plant Cell Physiol **43:** 384–392

Knoblach B, Sun X, Coquelle N, Fagarasanu A, Poirier RL, Rachubinski RA (2013) An ER-peroxisome tether exerts peroxisome population control in yeast. EMBO J **32:** 2439–2453

Lindeberg T (1994) Scale-Space Theory in Computer Vision. Kluwer Academic Publishers, Boston

Madison SL, Nebenführ A (2013) Understanding myosin functions in plants: are we there yet? Curr Opin Plant Biol **16:** 710–717

Mahamdeh M, Campos CP, Schäffer E (2011) Under-filling trapping objectives optimizes the use of the available laser power in optical tweezers. Opt Express **19:** 11759–11768

Mano S, Nakamori C, Hayashi M, Kato A, Kondo M, Nishimura M (2002) Distribution and characterization of peroxisomes in Arabidopsis by visualization with GFP: dynamic morphology and actin-dependent movement. Plant Cell Physiol **43:** 331–341

Mathur J, Barton KA, Schattat MH (2013) Fluorescent protein flow within stromules. Plant Cell **25:** 2771–2772

Mathur J, Mammone A, Barton KA (2012) Organelle extensions in plant cells. J Integr Plant Biol **54:** 851–867

Mathur J, Mathur N, Hülskamp M (2002) Simultaneous visualization of peroxisomes and cytoskeletal elements reveals actin and not microtubule-based peroxisome motility in plants. Plant Physiol **128:** 1031–1045

Mehrshahi P, Stefano G, Andaloro JM, Brandizzi F, Froehlich JE, DellaPenna D (2013) Transorganellar complementation redefines the biochemical continuity of endoplasmic reticulum and chloroplasts. Proc Natl Acad Sci USA **110:** 12126–12131

Murtagh F, Starck JL (2000) Image processing through multiscale analysis and measurement noise modeling. Stat Comput **10:** 95–103

Nieminen TA, Loke VLY, Stilgoe AB, Knoner G, Branczyk AM (2007) Optical tweezers computational toolbox. J Opt Pure Appl Opt **9:** S196–S203

Oikawa K, Kasahara M, Kiyosue T, Kagawa T, Suetsugu N, Takahashi F, Kanegae T, Niwa Y, Kadota A, Wada M (2003) Chloroplast unusual positioning1 is essential for proper chloroplast positioning. Plant Cell **15:** 2805–2815

Oikawa K, Matsunaga S, Mano S, Kondo M, Yamada K, Hayashi M, Kagawa T, Kadota A, Sakamoto W, Higashi S, et al (2015) Physical interaction between peroxisome and chloroplasts elucidated by *in situ* laser analysis. Nature Plants **1:** 15035

Oikawa K, Yamasato A, Kong SG, Kasahara M, Nakai M, Takahashi F, Ogura Y, Kagawa T, Wada M (2008) Chloroplast outer envelope protein CHUP1 is essential for chloroplast anchorage to the plasma membrane and chloroplast movement. Plant Physiol **148:** 829–842

Prestele J, Hierl G, Scherling C, Hetkamp S, Schwechheimer C, Isono E, Weckwerth W, Wanner G, Gietl C (2010) Different functions of the C3HC4 zinc RING finger peroxins PEX10, PEX2, and PEX12 in peroxisome formation and matrix protein import. Proc Natl Acad Sci USA **107:** 14915–14920

Prinz WA (2014) Bridging the gap: membrane contact sites in signaling, metabolism, and organelle dynamics. J Cell Biol **205:** 759–769

Sandalio LM, Romero-Puertas MC (2015) Peroxisomes sense and respond to environmental cues by regulating ROS and RNS signalling networks. Ann Bot (Lond) **116:** 475–485

Schattat M, Barton K, Baudisch B, Klösgen RB, Mathur J (2011) Plastid stromule branching coincides with contiguous endoplasmic reticulum dynamics. Plant Physiol **155:** 1667–1677

Scherp P, Hasenstein KH (2007) Anisotropic viscosity of the Chara (Characeae) rhizoid cytoplasm. Am J Bot **94:** 1930–1934

Schmidt von Braun S, Schleiff E (2008) The chloroplast outer membrane protein CHUP1 interacts with actin and profilin. Planta **227:** 1151–1159

Schnarrenberger C, Burkhard C (1977) In-vitro interaction between chloroplasts and peroxisomes as controlled by inorganic phosphate. Planta **134:** 109–114

Schumann U, Prestele J, O'Geen H, Brueggeman R, Wanner G, Gietl C (2007) Requirement of the C3HC4 zinc RING finger of the Arabidopsis PEX10 for photorespiration and leaf peroxisome contact with chloroplasts. Proc Natl Acad Sci USA **104:** 1069–1074

Scott I, Sparkes IA, Logan DC (2007) The missing link: inter-organellar connections in mitochondria and peroxisomes? Trends Plant Sci **12:** 380–381, author reply 381–383

Sinclair AM, Trobacher CP, Mathur N, Greenwood JS, Mathur J (2009) Peroxule extension over ER-defined paths constitutes a rapid subcellular response to hydroxyl stress. Plant J **59:** 231–242

Sparkes I (2011) Recent advances in understanding plant myosin function: life in the fast lane. Mol Plant **4:** 805–812

Sparkes I, Runions J, Hawes C, Griffing L (2009a) Movement and remodeling of the endoplasmic reticulum in nondividing cells of tobacco leaves. Plant Cell **21:** 3937–3949

Sparkes IA, Brandizzi F, Slocombe SP, El-Shami M, Hawes C, Baker A (2003) An Arabidopsis *pex10* null mutant is embryo lethal, implicating peroxisomes in an essential role during plant embryogenesis. Plant Physiol **133:** 1809–1819

Sparkes IA, Ketelaar T, de Ruijter NC, Hawes C (2009b) Grab a Golgi: laser trapping of Golgi bodies reveals in vivo interactions with the endoplasmic reticulum. Traffic **10:** 567–571

Sparkes IA, Runions J, Kearns A, Hawes C (2006) Rapid, transient expression of fluorescent fusion proteins in tobacco plants and generation of stably transformed plants. Nat Protoc **1:** 2019–2025

Sparkes IA, Teanby NA, Hawes C (2008) Truncated myosin XI tail fusions inhibit peroxisome, Golgi, and mitochondrial movement in tobacco leaf epidermal cells: a genetic tool for the next generation. J Exp Bot **59:** 2499–2512

Tamura K, Iwabuchi K, Fukao Y, Kondo M, Okamoto K, Ueda H, Nishimura M, Hara-Nishimura I (2013) Myosin XI-i links the nuclear membrane to the cytoskeleton to control nuclear movement and shape in Arabidopsis. Curr Biol **23:** 1776–1781

Thazar-Poulot N, Miquel M, Fobis-Loisy I, Gaude T (2015) Peroxisome extensions deliver the Arabidopsis SDP1 lipase to oil bodies. Proc Natl Acad Sci USA **112:** 4158–4163

Yang Y, Sage TL, Liu Y, Ahmad TR, Marshall WF, Shiu SH, Froehlich JE, Imre KM, Osteryoung KW (2011) CLUMPED CHLOROPLASTS 1 is required for plastid separation in Arabidopsis. Proc Natl Acad Sci USA **108:** 18530–18535